5-6-2004

Geomorphic Analysis of Tidal Creek Networks

Karyn Inez Novakowski

Raymond Torres

L Robert Gardner

George Voulgaris
University of South Carolina - Columbia, gvoulgaris@geol.sc.edu

Publication Info

Published in *Water Resources Research*, Volume 40, Issue W05401, 2004, pages 1-13.
Novakowski, K. I., Torres, R., Gardner, L. R., & Voulgaris, G. (2004). Geomorphic analysis of tidal creek networks. *Water Resources Research, 40* (W05401), 1-13.

Geomorphic analysis of tidal creek networks

Karyn Inez Novakowski, Raymond Torres, L. Robert Gardner, and George Voulgaris
Department of Geological Sciences, University of South Carolina, Columbia, South Carolina, USA

Received 2 October 2003; revised 7 January 2004; accepted 26 January 2004; published 6 May 2004.

[1] The purpose of this study is to determine if concepts in terrestrial channel network analysis provide insight on intertidal creek network development and to present new metrics for their analysis. We delineated creek network geometry using high-resolution digital images of intertidal marsh near Georgetown, South Carolina. Analyses reveal that intertidal creek networks may be topologically random. Length-area relationships suggest that salt marsh and terrestrial networks have similar scaling properties, although the marsh networks are more elongate than terrestrial networks. To account for recurrent water exchange between creek basins at high tide, we propose that the landscape unit of geomorphic analyses should be the salt marsh island as opposed to salt marsh creek drainage basin area. Using this approach, the relationship between maximum channel length per island and island area is well described by a power function. A similar power relationship exists for cumulative channel length versus island area, giving a nearly unit slope; this implies that marsh islands have a spatially uniform drainage density. Since the island boundaries are easily identified in remote sensing, taking the island as the unit of geomorphic analysis will eliminate discrepancies in delineating basin boundaries and preclude the need for defining basin area in intertidal landscapes. Analyses and results presented here may be used to quantify salt marsh reference condition and provide indicator variables to assess salt marsh disturbance. *INDEX TERMS:* 1824 Hydrology: Geomorphology (1625); 1848 Hydrology: Networks; 1640 Global Change: Remote sensing; *KEYWORDS:* drainage areas, geomorphology, islands, networks, salt marsh

Citation: Novakowski, K. I., R. Torres, L. R. Gardner, and G. Voulgaris (2004), Geomorphic analysis of tidal creek networks, *Water Resour. Res.*, *40*, W05401, doi:10.1029/2003WR002722.

1. Introduction

[2] Estuarine and intertidal environments are sediment sinks with complex hydrodynamic processes that produce spatially variable deposition and erosion [e.g., *Pestrong*, 1965; *Leonard*, 1997; *Fagherazzi and Furbish*, 2001]. Sediment accumulation leads to mudflat formation, with salt marsh at higher elevations [*Redfield*, 1972; *Allen and Pye*, 1992]. Typically, tidal creek networks etch the salt marsh surface, becoming dry at low tide. These small-scale channels facilitate inundation and drainage of marshlands and they control, to a large extent, estuary-wide hydrodynamics [*Pestrong*, 1965; *Rinaldo et al.*, 1999a]. Moreover, marsh channel networks control mass and energy exchange with the coastal ocean and therefore help sustain high salt marsh productivity; they also provide critical habitat for economically important fish. Hence salt marsh landscapes are the geographic templates upon which highly productive intertidal ecosystems function, and in order to understand the development and stability of salt marsh systems an improved understanding of salt marsh landforms is required.

[3] Early work on intertidal zone geomorphology was focused on the hydraulic geometry of estuarine channels. Results from these efforts indicate that intertidal channels exhibit an exponential decrease in width in the upstream direction, and that this change in geometry facilitates greater tidal energy dissipation through the channel network by increased friction [*Myrick and Leopold*, 1963; *Langbein*, 1963; *Wright et al.*, 1973]. *Pestrong* [1965] favors the *Horton* [1945] model of channel development for intertidal channels with the important distinction that marsh incision occurs during the higher velocity ebb flows. Pestrong also recognized that microtopography may control channel initiation by concentrating sheet flow, and some tributaries may experience predominantly unidirectional flow. He went on to reason that some channels be characterized as terrestrial, influenced by their contributing areas.

[4] Subsequent marsh geomorphic research has focused on planform geometry. *Geyl* [1976] attempted to link channel network characteristics to tidal channel basin area. He used air photos and small-scale maps to characterize the stability of channel networks. Although the main findings are inconclusive, Geyl's analyses represent an early attempt at using drainage basin area to compare terrestrial and estuarine channel networks.

[5] *Wadsworth* [1980] conducted detailed studies of drainage density and channel reticulation in the tidal Duplin River system. Like *Geyl* [1976], Wadsworth used these analyses to infer marsh network stability. Wadsworth reasoned that network boundary conditions and local slope are primary controls on network evolution, and that channel length is more responsive to tidal forcing than contributing area of the individual tidal basins. *Collins et al.* [1987] presented the first detailed description of marsh morphology by evaluating the topography of a 4.5 ha section of marsh

0043-1397/04/2003WR002722

area within the 30 km^2 Petaluma River Estuary. They found that biogenic and physical processes interact and are in delicate equilibrium with marsh morphology. They also reasoned that tidal prism continuity drives geomorphic evolution in marsh landscapes, and went on to infer that terrestrial concepts of drainage basin evolution apply to intertidal marsh environments. They did not, however, use terrestrial geomorphic indices to evaluate marsh geomorphology (e.g., contributing area - channel length).

[6] *Pethick* [1992] reasoned that salt marshes should be regarded as the landward extension of mudflat systems, and that salt marshes self-adjust in response to storm perturbations. *Pethick* also suggested that some marsh channels may have resulted from flood tide inundation, as opposed to the ebb tide drainage model of *Pestrong* [1965]. These findings may underlie the observation by *Marani et al.* [2003] that drainage density is not a diagnostic feature of salt marsh landscapes.

[7] Despite the vastly different environmental conditions, field observations reveal that intertidal channel networks bear a strong resemblance to those of terrestrial systems [e.g., *Pestrong*, 1965; *Knighton et al.*, 1992; *Pethick*, 1992]. *Cleveringa and Oost* [1999] support this contention by providing evidence for "statistical self-similarity" in tidal basin channel networks, a common feature of terrestrial channel systems. On the other hand, *Ragotzkie* [1959] observed that marsh basin networks in a region of uniform tidal range were highly variable. This general finding is supported by *Fagherazzi et al.* [1999]; their nonlinear plots of marsh basin area-channel length indicate that tidal channel networks are not scale-invariant, unlike most terrestrial channel networks.

[8] Typically, landscape evolution models assume that landscape forming discharges (Q) are proportional to the watershed contributing area (A) that is defined by topography (i.e., $Q \propto A$). *Rinaldo et al.* [1999a] used a linearized version of the governing flow equations to model water surface topography during high tide. They exploited the $Q \propto A$ assumption by redefining the contributing areas using flow divides associated with the free water surface (energy slope) rather than area defined by topography of tidal basins. *Rinaldo et al.* [1999a] used their model results to test for scale invariance and they concluded that terrestrial models of geomorphic evolution do not apply to tidal basin geomorphology.

[9] Subsequently, *Rinaldo et al.* [1999b] tested for scale invariance by linking water surface topography to maximum discharge as estimated by the linearized hydrodynamic model. They found power law relationships between channel cross-sectional area, drainage area, tidal prism and peak discharge at spring tides. However, their power law models hold only for larger channels with a cross-sectional area greater than 50 m^2; below that the power law relationship does not apply. This finding was attributed to inadequate spatial resolution of the digital terrain model, and to the assumptions included in their hydrodynamic modeling that made it inappropriate for smaller channels. *Fagherazzi and Furbish* [2001] suggested that the break in the power law scaling is the result of increased sediment shear resistance with substrate depth. In their work on the intertidal channel networks of the Venice Lagoon, *Marani et al.* [2003] found that there are regional differences in the dependence of total channel length on the volume of the tidal prism but uniformity in the correlation of total channel length with watershed area. These findings led them to suggest that the volume of the tidal prism is not a major control on channel network geometry.

[10] Together these studies reveal that a consensus on the role of hydrodynamic processes on intertidal geomorphology, scaling of geomorphic features, and what constitutes intertidal basin boundaries is lacking. Here, we quantify the planform geomorphic properties of intertidal channel patterns using high-resolution (0.7 m $\times$ 0.7 m) digital imagery. The purpose of this study is to determine if concepts in terrestrial channel network analysis provide insight on intertidal creek network structure and development, to present new metrics for their analysis, and to evaluate randomness in network topology. This latter goal is important because a positive result may establish a foundation for using terrestrial concepts in the intertidal zone. Moreover, geomorphic metrics evaluated in this study may be used to guide salt marsh reconstruction efforts and serve as indicators for marsh disturbance.

[11] Here basin and network analyses are limited to those landscapes wholly within the intertidal zone, the small-scale drainage basin areas that do not intersect the terrestrial landscape. This distinction is important because we endeavor to evaluate the effects of recurrent tidal forcing and subsequent material fluxes on salt marsh geomorphology (and to a lesser extent the effects of low tide rainfall events [e.g., *Torres et al.*, 2003]). Although results presented here may be site specific, the analyses and main findings may provide a framework for salt marsh landscape analysis that apply to other intertidal environments.

2. Study Site

[12] The study area is in the North Inlet estuary, located near Georgetown, South Carolina (Figure 1). This estuary-marsh-forest system is part of the National Estuarine Research Reserve System (NERRS). North Inlet is a 32 km^2 bar-built, ebb-dominated, relatively pristine lagoonal estuary with extensive salt marsh, and mean tidal range of 1.5 m [*Gardner and Porter*, 2000]. The tide is modestly asymmetric with a flood tide duration of 6.5 to 7.0 hours and an ebb duration of 5.5 to 6.0 hours. As a result the peak ebb velocities ($\sim$1.5 m/s) are larger than peak flood velocities. The climate is subtropical with average monthly temperatures between 9–27°C, and annual rainfall of approximately 1.4 m with frequent high intensity, low duration cyclonic and convective storms (National Climatic Data Center COOPID 383468). The northern perimeter of the marsh is bounded by a residential development. Mud Bay lies to the south and it is an embayment of the larger Winyah Bay, an estuary that receives freshwater input from the Pee Dee River. To the east of the marsh is a Holocene barrier beach system whereas Pleistocene beach ridges, oriented northeast-southwest, border the salt marsh to the west. With the exception of the northern most edge, the area around North Inlet estuary is held in conservation. *Spartina alterniflora* is the dominant vegetation in the salt marsh, but other vegetation includes *Salicornia virginica* and *Juncus romerianus* at higher elevations.

[13] Sediment budget studies show that North Inlet is a sediment sink, importing fine suspended sediment from the

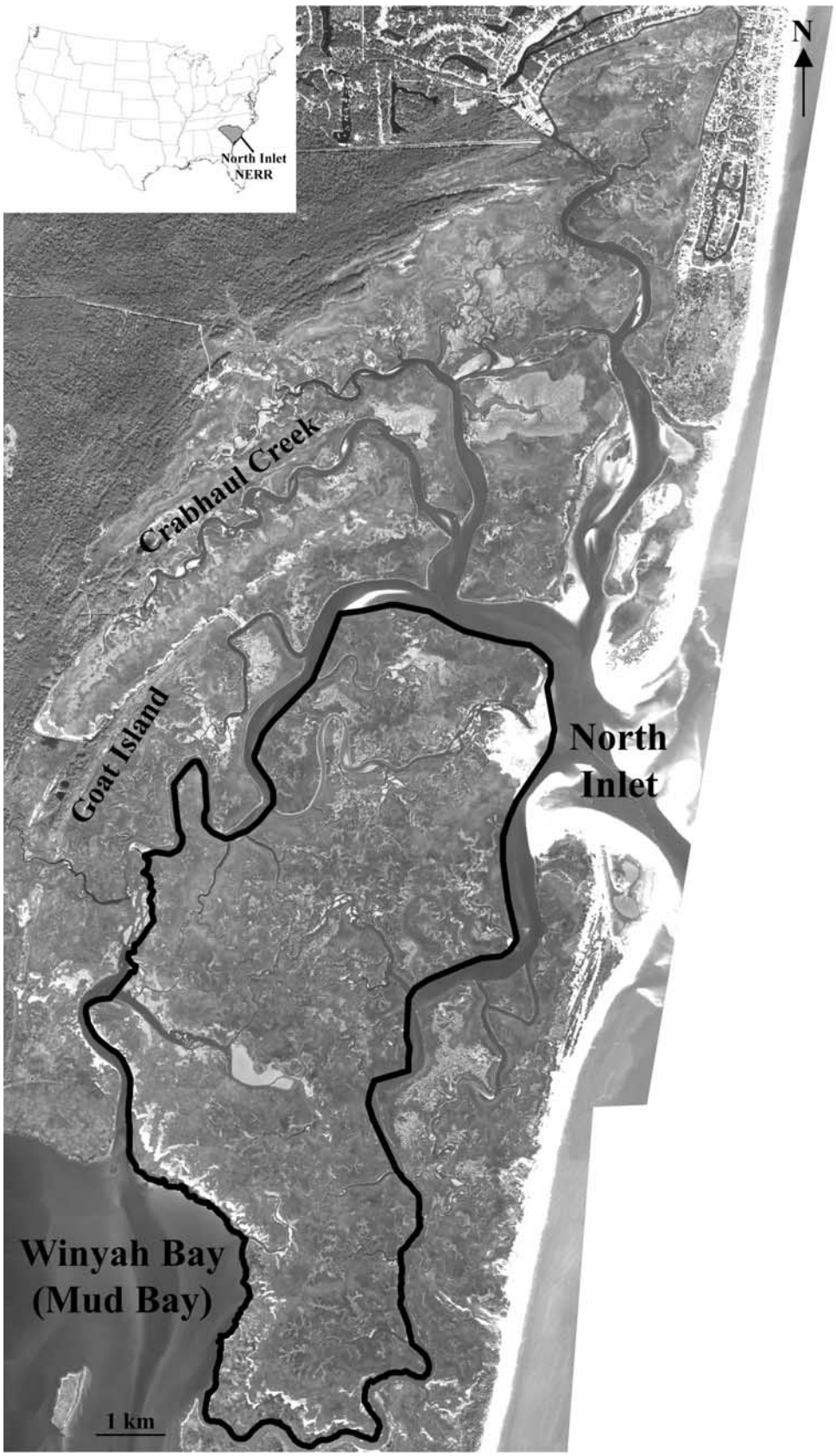

Figure 1. ADAR image shows location and geography of North Inlet. The study area is outlined in black. See color version of this figure at back of this issue.

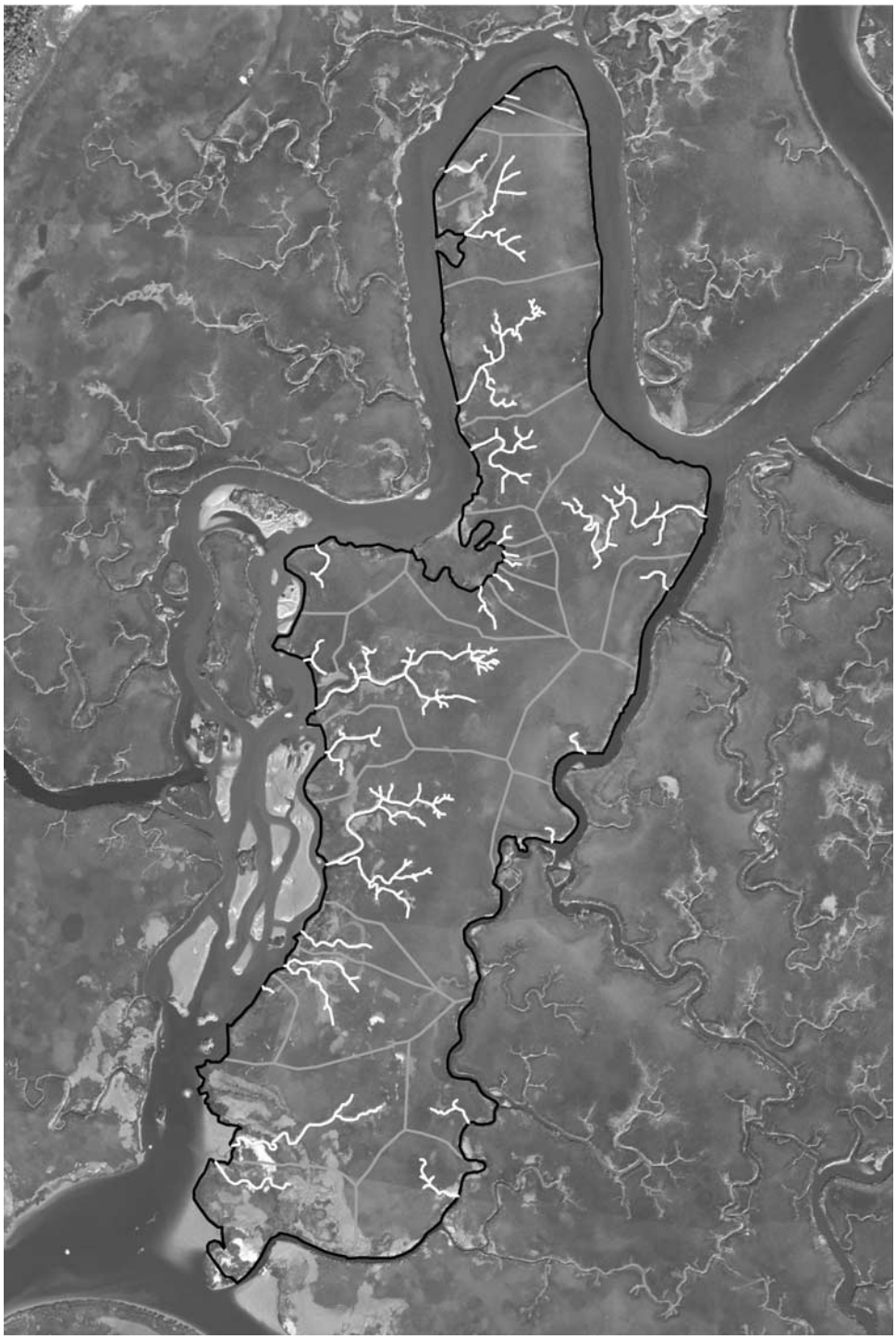

Figure 2. ADAR image showing an intertidal island outlined in black, creeks shown in white, and watershed boundaries shown in gray.

Atlantic Ocean and Winyah Bay [*Gardner et al.*, 1989; *Vogel et al.*, 1996]. The inorganic fraction accounts for 80–85% of the accumulating mass [*Gardner and Kitchens*, 1978; *Vogel et al.*, 1996]. The organic fraction (15–20%) is derived from a variety of sources that include remains of algae, animals, microbes, terrestrial vegetation and marsh plants [*Goñi and Thomas*, 2000], the latter mainly *S. alterniflora*. ^{137}Cs analyses show that local annual average sediment accumulation rates range from 1.3–2.5 mm/yr [*Sharma et al.*, 1987]. This accumulation rate is comparable to the local sea level rise rate of 2.2–3.4 mm/yr; hence the marsh surface is rising with sea level [*Vogel et al.*, 1996].

[14] The extensive salt marsh system has numerous well-defined tidal channel networks that dissect the marsh surface (Figure 2). Typically, the deeper and wider tidal channels do not drain completely at low tide and may circumscribe salt marsh islands, and each marsh island may contain several networks and associated watersheds.

These smaller channel networks incise the marsh platform and become "dry" at low tide. The analyses presented here are focused on the latter, smaller scale salt marsh creek networks, excluding the marsh creek networks that extend into purely terrestrial environments. Therefore this research effort is directed at quantifying metrics for intertidal landscapes with recurrent marine forcing.

3. Methods

[15] The base image for this study was acquired with an Airborne Data Acquisition and Registration (ADAR) 5500 digital camera system with multispectral (blue, green, red, near IR) band widths (Figure 1). The image was obtained on November 4, 1999 from an altitude of 2763 m, close to solar noon and low tide to limit sun angle and tidal inundation effects, yielding a spatial resolution of approximately 0.7 × 0.7 m [*Jensen et al.*, 2002]. Creek networks (Figure 2) were delineated by visually comparing percent reflectance of *S. alterniflora*, water, and the gray to black, organic rich marsh mud. Water absorbs incident light reflecting 0–4%, marsh grass 5–50%, and mud 15–20% [*Jensen*, 2000]. Reflectance differences between grass, water, and marsh mud facilitates the delineation of the channel networks on the marsh surface. Typically, the creek bed and inner banks are devoid of vegetation thereby facilitating delineation of the mid-channel. Field observations at low tide reveal that tidal creek networks that etch the marsh platform typically do not have flowing water greater than a few millimeters depth or a few centimeters of standing water, or they may be completely dry. These tidal creeks are distinct from the larger tidal channels that typically retain >1 m of standing water at low tide and thereby form salt marsh islands.

[16] Analyses show that most creek networks, those becoming "dry" at low tide, are ideal in the sense that they have no lakes, islands, or junctions with more than two tributaries. Some networks, however, were not delineated and excluded from further analysis because they contained reticulating drainage systems, thereby precluding use of conventional terrestrial network metrics. Reticulating creek networks diverge in the downstream direction and later rejoin [*Wadsworth*, 1980]. The following properties were determined for each segment of each non reticulating creek network, in ArcView: link length (l) and link magnitude (μ, where link refers to a first order stream segment), Strahler stream order (ω), maximum stream length (L, the longest stream from the outlet to the source point), total channel length (ΣL), watershed area (A_w) and island area (A_I). We also evaluated the frequency of topologically distinct creek network types [e.g., *Shreve*, 1974].

[17] A topologically random network is a network in which all topologically distinct sub-networks of equal magnitude occur with equal probability [*Shreve*, 1974]. The number of topologically distinct networks for a given number of sources, is given by

$$N(M) = \frac{(2M-2)!}{M!(M-1)!} \quad (1)$$

where M is the number of sources. Randomness was tested by counting the number of times that each topologically distinct sequence occurred and comparing it to the expected value using a chi-squared (χ^2_α) test where $\alpha = 0.05$, degrees of freedom = $k - 1$, where k is the number of categories. A χ^2 test is a measure of how much an observed value deviates from an expected value. Here it is assumed that networks are topologically random if each possible sequence occurred with equal probability, or expected values equaled observed values. If $\chi^2_{observed}$ is greater than χ^2_α then the hypothesis that marsh creek networks are topologically random is rejected.

[18] As described above, an island is a section of marsh circumscribed by tidal channels that maintain >1 m of water at low tide. Island boundaries were identified in the same manner as tidal creeks, visual inspection of reflectance between marsh grass and mud in surrounding channels. Island areas (A_I) were then determined with ArcView. Watershed area (A_w) is that area encompassing an individual, discrete creek network. Watershed areas were determined by a Theissen polygon method using end points of first order creeks, essentially assuming the watershed boundary is one half the distance between end points of first order creeks in neighboring basins, and mid points between adjacent creek mouths. The Theissen polygon results were compared to results from manually delineating watershed boundaries for 22 creek networks on a marsh island (Figure 2). The graphical comparison has a slope of 0.95 and $r^2 = 0.96$, indicating that there is not a significant difference between the two methods. Therefore the automated method was used to avoid ambiguity in A_w delineation.

4. Results

[19] The study area is an 8.67 km^2 portion of the North Inlet intertidal marsh (Figure 1). In this mapped region the deeper and wider intertidal channels retain water at low tide, and consequently circumscribe 56 marsh islands. We delineated the intertidal channel networks on these islands; there were 725 in total. Maximum channel lengths and associated network watershed areas ranged from 3 m to 10654 m, and 127 m^2 to 609418 m^2, respectively. Approximately 94% of the networks had a terrestrial network appearance; this means that in the downstream direction, channel segments converge toward a main channel. On the other hand, approximately 9.1 km or 6% of total channel length was classified as being part of a reticulating drainage system.

4.1. Stream Order

[20] The nonreticulating networks were less than or equal to Strahler stream order 5 (Table 1). Total number of stream segments decline exponentially from 3254 first order segments to 20 of order 5. Applying Horton's laws of drainage composition, order (ω) versus number of stream and mean stream length (l_m) reveals an exponential trend that is similar to those found in terrestrial systems. Figure 3 contains data from this study together with data from eight other studies, three from terrestrial systems and five from the coastal zone. Some of the terrestrial and intertidal trends in these data overlie each other despite differences in scale from which the data points were extracted and processes controlling network development. The logarithmic relationship is $y = Ae^{B\omega}$ where y is the number of channels of a given order, and ω is stream order, A is the y intercept, and B is the slope of the line (Table 2). The minimum correlation

Table 1. Count, Sum, and Mean Stream Lengths for a Given Order for All Networks

Order	Length Count	Total Length, m	Mean Length, m
1	3254	58588	18 ± 16
2	1613	42749	26 ± 34
3	614	22938	37 ± 37
4	145	6833	47 ± 43
5	20	1049	52 ± 32

coefficient, r^2, for these curve fits is 0.95 (data from North Inlet). These high correlation coefficients indicate that the exponential model adequately describes changes in stream frequency with order.

[21] Mean stream segment length exponentially increases with order (Horton's law of stream order) although there are distinct differences in the trends between terrestrial and coastal networks (Figure 4). For example, the terrestrial data illustrate a nearly uniform positive slope and higher r^2 values (Table 2). The coastal data on the other hand are different in two ways. First, the *Wadsworth* [1980], *Pestrong* [1965], and *Pethick* [1980] data show a uniform slope between orders 1–4, well described by an exponential function, with slopes comparable to the terrestrial systems (Table 2). At order 5 however, there is an abrupt break in slope due to a lower than expected channel length. This low value for mean channel length may be due to under sampling of order 5 channels. For example, Pestrong reports 4 order 5 channels and both Wadsworth and Pethick have 1 order 5 channel. Secondly, the slope of the *Myrick and Leopold* [1963] data is greater than the terrestrial trend slope, while the slope for the North Inlet data is lower. Together these data show that mean channel length is highly variable. Also, these exponential relationships (Figures 3 and 4) are consistent with Horton's law of stream numbers and lengths, and they are consistent with expectations from *Kirchner* [1993] who showed that Horton ratios are insensitive to network structure.

Table 2. Summary of Slope B Values of Marsh and Terrestrial Networks for the Function $y = Ae^{B\omega}$

Study	B_{count}	r^2_{count}	$B_{mean\ length}$	$r^2_{mean\ length}$
North Inlet	−1.23	0.95	0.27	0.94
Wadsworth [1980]	−1.31	0.99	0.25 (−0.79)	0.09 (−0.95)
Pestrong [1965]	−1.35	0.99	0.73 (−1.0)	0.48 (−0.99)
Myrick and Leopold [1963]	−1.08	0.97	1.33	0.99
Pethick [1980]	−1.33	0.99	0.38 (−0.79)	0.13 (−0.95)
Zeff [1999]	−1.27	0.99	1.01	0.99
Brush [1961]	−1.20	0.99	1.01	0.99
Valdes et al. [1979]	−1.25	0.99	0.89	0.98
Horton [1945]	−1.22	0.99	0.76	0.92

4.2. Link Magnitude

[22] Discrete channel networks had link magnitudes (μ) ranging from 1 to 229 (Table 3), with a total of 3254 magnitude 1 channels comprising 58.6 km, and 896 magnitude 2 channels comprising 20.8 km. Therefore magnitude 1 channels comprise 57% of all channels, and 45% of total channel length, magnitude 2 channels comprise 16% and 16%, respectively. As *Shreve* [1969] noted and *Kirchner* [1993] confirmed, stream order analyses (e.g., Horton laws) lack sensitivity to detect substantial differences in geomorphic character. As a consequence, we propose that semilogarithmic plots of magnitude versus frequency and mean channel length may yield insight on systematic variations in network structure.

[23] Figure 5 shows that stream frequency declines as a power function from magnitude 1 to magnitude 33, but thereafter scatter about the curve fit increases substantially. Also, over the range of magnitude 34 to 93 there are 14 link magnitude values that have a single occurrence, and 12 channel networks with magnitude >93 have a single occurrence. On the other hand, mean channel length shows an increase over the same range in magnitude, but the scatter

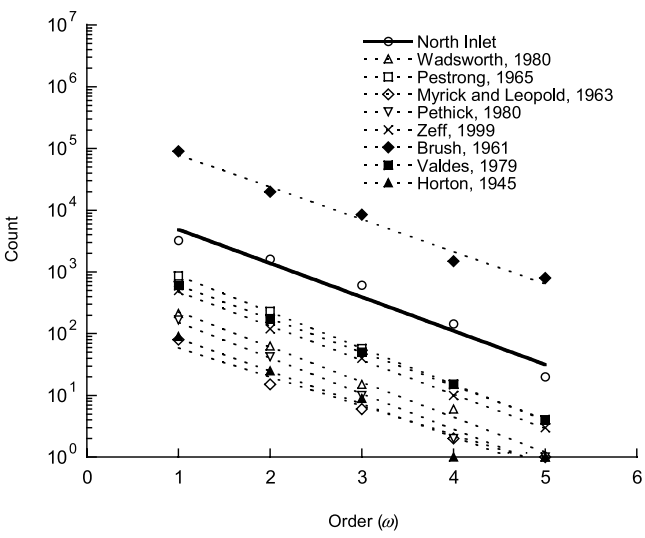

Figure 3. Stream order (ω) versus the number of streams for terrestrial and marsh networks (Horton's law of stream numbers). Marsh data are open symbols, and terrestrial data are solid symbols.

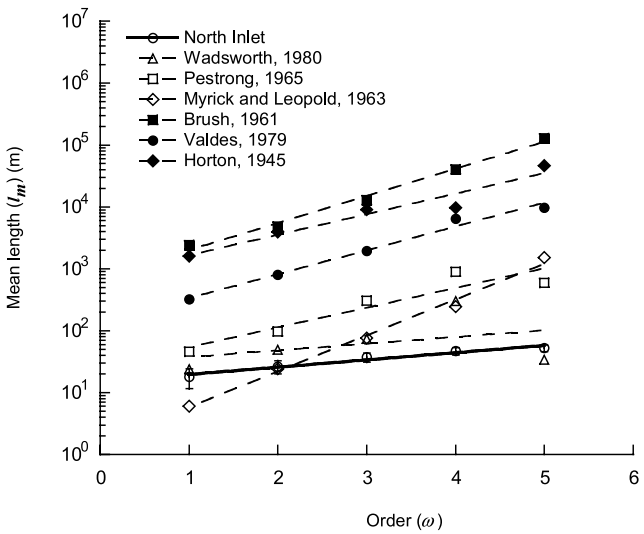

Figure 4. Stream order (ω) versus the mean segment lengths (l_m) for marsh and terrestrial networks (Horton's law of stream lengths). Marsh data are open symbols, and terrestrial data are solid symbols. Standard errors on each mean value are represented by error bars.

Table 3. Count and Sum of Link Lengths for a Given Magnitude

Magnitude, μ	Length Count	Total Length, m	Cumulative Percent	Mean Length, m
1	3254	58588	44.3	18
2	896	20774	60.1	23
3	384	10505	68	27
4	235	7058	73.4	30
5	151	6046	77.9	40
6	102	3786	80.8	37
7	91	2892	83	31
8	70	2662	85	38
9	61	2650	87	43
10	49	1822	88.4	37
11	33	1148	89.3	34
12	40	1521	90.4	38
13	27	1164	91.3	43
14	20	1011	92.1	50
15	18	682	92.6	37
16	16	594	93	37
17	15	856	93.7	57
18	8	357	93.9	44
19	9	288	94.2	32
20	11	352	94.4	32
21	10	460	94.8	46
22	10	352	95	35
23	11	476	95.4	43
24	7	175	95.5	25
25	6	196	95.7	32
26	15	785	96.4	52
27	9	388	96.6	43
28	5	181	96.7	36
29	5	246	96.9	49
30	5	267	97.1	53
31–229	72	3840	100	51

about the curve fit increases substantially after magnitude 33. Channel segments of magnitude 1–6 comprise 81% of total channel length and 89% of total channel segments counted. The rate of change in mean channel length, however, decreases to ~1 m per increase in magnitude between magnitude 6 to magnitude 17, but the scatter about the curve fit increases substantially at greater magnitude (Figure 5). This trend indicates that a "limit" to mean channel length, or distance between tributaries, may exist in networks with link magnitude 6 to 17.

[24] The topologically random network model developed by *Shreve* [1966] and *Smart* [1968] provides the theoretical framework for the prediction of drainage network composition (e.g., Horton's and Hack's laws). As *Shreve* [1974] stated, a topologically random population of channel networks is one in which all topologically distinct channel networks of the same magnitude are equinumerous. Random topology in North Inlet salt marsh creek networks was evaluated using the equinumerous test. We evaluated the occurrence of each possible topological sequence for a given magnitude (Table 4). Of course, magnitude 1 and magnitude 2 networks have one possible sequence for each. There are 325 magnitude 3 networks; given that there are only two possible sequences for magnitude 3 the expected occurrence of each is 162.5; there were 172 and 153 occurrences of each network sequence, respectively. For magnitude 4 networks there are 5 possible sequences. The total number of magnitude 4 networks is 194, with an expected value of 38.8. There were counts of 43, 45, 32, 41, and 33 for all possible network sequences. Fourteen possible sequences exist for magnitude 5 networks and a total of 115 magnitude 5 networks with an expected value for magnitude 5 sequences of 8.2. Counts of 10, 9, 7, 6, 10, 10, 11, 7, 4, 5, 10, 10, 8, and 8 exist for the magnitude 5 sequences. To compare expected values to observed values chi-squared test for goodness-of-fit of observed to expected counts were performed (Table 4). All χ^2 values are less than the χ^2_α, therefore for magnitudes 3, 4, and 5 we cannot

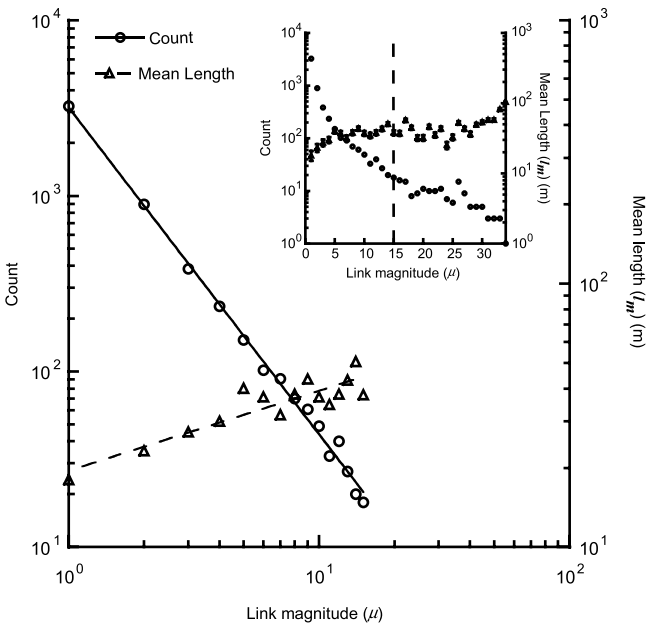

Figure 5. Magnitude (μ) versus number of creek segments and the mean length (l_m) for μ_{1-15}. Inset shows relationship for μ_{1-33}. Vertical line indicates where scatter increases significantly. Standard errors on each mean value are represented by error bars.

Table 4. Count of Sequence Magnitudes and Chi Square Values[a]

μ	Sequence	Count	Test Statistic
3	IEIEE	172	0.56
3	IIEEE	153	0.56
4	IEIEIEE	43	0.45
4	IIEEIEE	45	0.99
4	IEIIEEE	32	1.19
4	IIEIEEE	41	0.12
4	IIIEEEE	33	0.87
5	IEIEIEIEE	10	0.39
5	IIEEIEIEE	9	0.08
5	IEIIEEIEE	7	0.18
5	IEIEIIEEE	6	0.59
5	IIEIEEIEE	10	0.39
5	IIEIEEIEE	10	0.39
5	IIEEIIEEE	11	0.95
5	IEIIEIEEE	7	0.18
5	IEIIIEEEE	4	2.16
5	IIEIEIEEE	5	1.26
5	IIEIIEEEE	10	0.39
5	IIIEIEEEE	10	0.39
5	IIIIEEEEE	8	0.01
5	IIIEEEIEE	8	0.01

μ	Total Number	Expected	χ^2 Observed	$\chi^2_{0.05}$
3	325	162.5	1.11	3.84
4	194	38.8	3.63	9.49
5	115	8.2	7.35	22.36

[a]I is interior link, and E is exterior link.

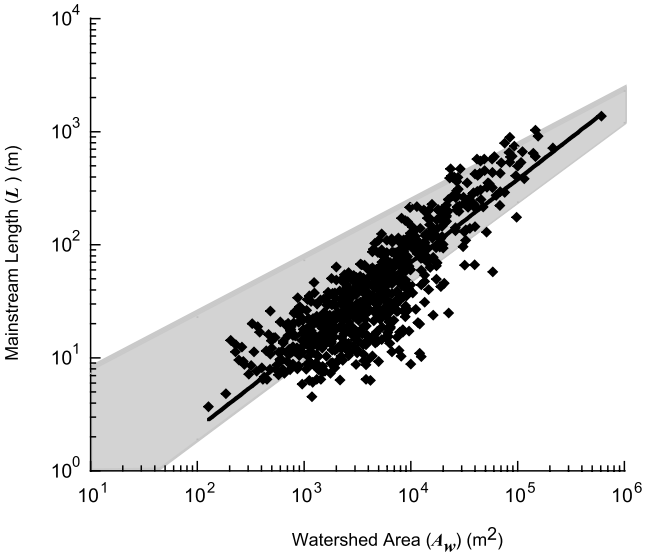

Figure 6. Mainstream length (L) versus watershed area (A_w). Regression equation $L = 0.08A_w^{0.73}$, $r^2 = 0.79$. Marsh data are shown as black diamonds. Terrestrial range is shown in gray [*Willemin*, 2000].

reject the hypothesis that marsh creek networks are topologically random.

4.3. Hack's Law

[25] For topologically distinct channel networks the length-area (L-A_w) relationship determined by *Hack* [1957] is expected from theoretical predictions by *Shreve* [1974]. L-A_w analyses for 725 nonreticulating channel networks were conducted (solid diamonds in Figure 6). The data vary over four orders of magnitude in watershed area A_w, and three orders of magnitude in mainstream length L. Scatter in the data declines with increasing basin area. A regression line through the L-A_w data with a correlation coefficient (r^2) of 0.79, gives the power function relation of $L = 0.08A_w^{0.73}$. For comparison to terrestrial systems, these data are plotted over a shaded region that depicts the upper and lower limits of terrestrial values for slope and y intercept reported in the literature, and projected to our scale of observation. In this case, *Willemin* [2000] defines these upper and lower limits, with y intercepts and slopes of 2.3 and 0.5 and 0.073 and 0.60, respectively. Approximately 86% of North Inlet marsh data fall within the range of the reported terrestrial values. Most of the data that lie outside of the terrestrial region lie below the terrestrial lower limit. The regression line, however, falls completely within the terrestrial region. Hence the intertidal creek networks and accompanying watershed areas appear to adhere to L-A_w relations postulated by *Hack* [1957] and predicted by *Shreve* [1974].

[26] Field observations show that well-developed and discrete channel networks and basin areas develop, and persist in intertidal environments. During tidal inundation when water may be exchanged between discrete tidal basins, exact basin or watershed boundaries defined by topographic highs are irrelevant to geomorphic analysis. Hence topographic flow divides, a well-established feature of terrestrial landscapes, typically do not exist in intertidal landscapes. Consequently, we developed an alternative procedure to further refine the Hack relationship in the intertidal zone; the procedure is based on island area as opposed to basin area. We propose that in some intertidal environments, the unit of geomorphic analysis should be the island instead of the watershed or basin. Using this approach, a semilogarithmic plot of island area (A_I) as the dependent variable against maximum mainstream length (L_{max}) of an island, for all 56 islands (Figure 7) are related by the power function $L = 0.11A^{0.65}$. These data exhibit a power function relationship that is similar to the Hack relationship for terrestrial landscapes, with a correlation coefficient (r^2) of -0.77.

4.4. Island Shape

[27] Here the question is: What is the effect of island shape on network geometry? This is important because we assume that marsh island shape will provide constraints on network dimension and geometry; that is, the island periphery is a landscape boundary. First, in order to quantify the variability in island shape a ratio of island area to area of a circumscribing circle was developed (A'). The closer A' is to 1 m the greater the island fills the circular space. The area ratio for all 56 islands ranges from 0.16 to 0.65 with a mean of 0.39 ± 0.12.

[28] The effect of island shape on maximum mainstream length was evaluated for each of the 56 islands. Maximum mainstream length ranges from 8 m to 1372 m with a mean of 222 ± 293 m. The majority (55%) of the lengths fall between 0 and 100 m, giving a right skewed distribution. Observations indicate that mainstreams tend to be oriented perpendicular to the long axis of elongate islands (Figure 2). We expect the relationship between A' and L_{max} to be positively correlated because islands with small area ratio values (elongate islands) most likely contain shorter mainstream lengths, while islands with a larger area ratio (more circular islands) should have longer mainstream lengths. Plots of these data (Figure 8), however, do not reveal any particular trend, and an exponential curve fit shows a weak positive correlation. The data also show that a single value

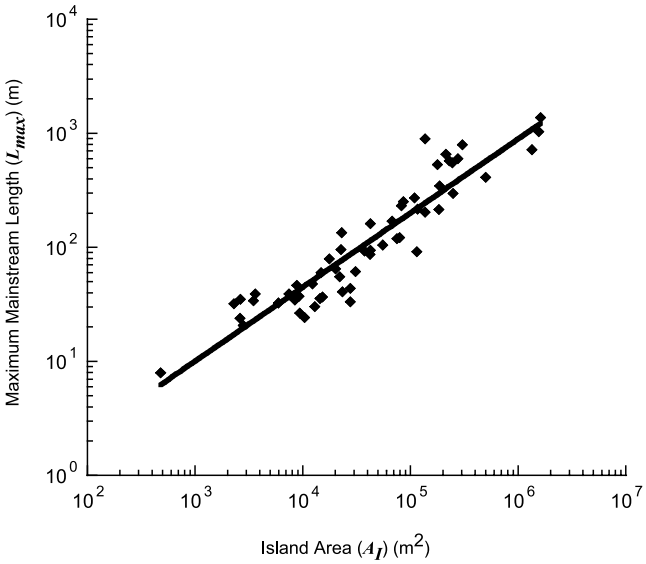

Figure 7. Maximum mainstream length (L_{max}) for a given island versus island area (A_I). Regression equation $L_{max} = 0.11A_I^{0.65}$, $r^2 = 0.77$.

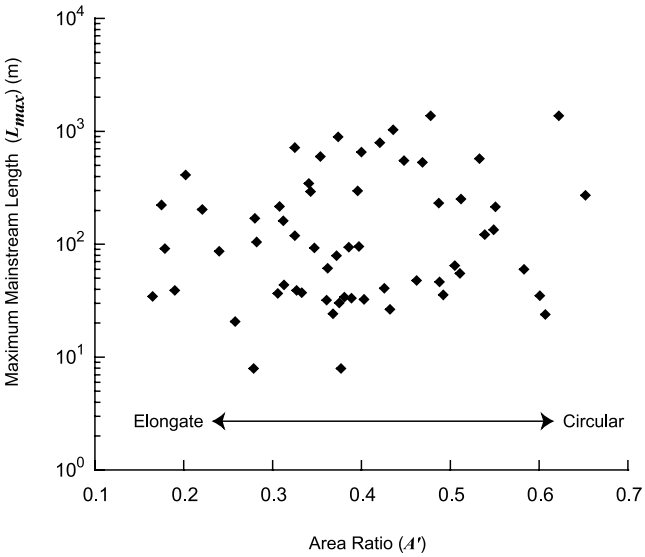

Figure 8. Maximum mainstream length (L_{max}) for each island versus area ratio (A').

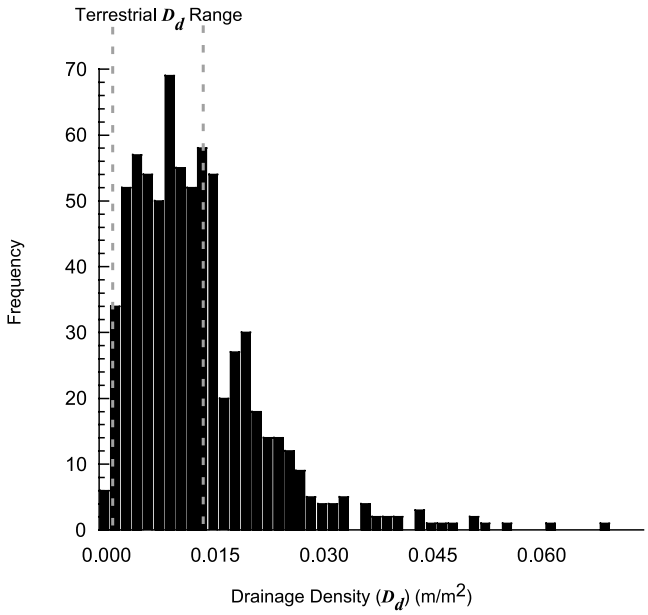

Figure 9. Drainage density (D_d). Dashed vertical lines contain the terrestrial range of D_d values.

of the area ratio does not have a well-constrained range of maximum mainstream lengths. Examining the effect of the area ratio on total stream length for each island reveals a similar lack of correlation. Moreover, subdividing the data in Figure 8 by island area shows that these findings persist. Together these observations show that island shape, and therefore boundaries have a negligible effect on network dimensions.

4.5. Drainage Density

[29] Drainage density, D_d, is defined as $\Sigma l/A$, where Σl = total channel length of the region of interest, and A = the corresponding area of the region. Total channel length in the 8.67 km^2 area was 113.7 km, giving a regional drainage density of 13.1 km/km^2 (0.013 m/m^2). The average drainage density for all 56 marsh islands was 0.012 ± 0.005 m/m^2, with a range of 0.003 m/m^2 to 0.021 m/m^2. The corresponding total channel lengths for islands ranged from 8 m to 28405 m, and island areas ranged from 482 m^2 to 1613547 m^2. Drainage density values for all 725 marsh watersheds range from 0.0008 m/m^2 to 0.069 m/m^2 with an average value 0.013 ± 0.009 m/m^2 (Figure 9). The corresponding watershed areas and total channel lengths range from 127 m^2 to 609418 m^2, and 4 m to 10654 m, respectively. For comparison, some terrestrial drainage density values range between 0.0023–0.0137 m/m^2 [*Ritter et al.*, 1995]; 57% of the marsh drainage density values fall within this terrestrial range (Figure 9). It is important to note the effect of map scale on drainage density calculations [*Gardiner et al.*, 1977; *Tucker et al.*, 2001] because stream lengths and areas determined on large scale maps may only include larger streams while neglecting the smaller tributaries. This may result in an underestimation of the total length for a given area, and therefore artificially low values of drainage density. The North Inlet drainage density data were collected on an image with 0.7 m spatial resolution. Because of this fine scale it is unlikely that a significant number of creek segments in a given area were overlooked. If the terrestrial data were collected on finer scale maps the terrestrial drainage density range might widen, possibly including more of the marsh drainage density values.

[30] *Pethick* [1992] hypothesized that intertidal drainage density is inversely related to watershed area. This relationship is supported by the intuitive argument that a plot of drainage density versus basin area amounts to a plot of A^{-1} versus A, giving rise to an inverse relation. These data show a great degree of variability in drainage density for a given watershed area. The relationship between total length for each creek network plotted against watershed area can reveal specific information about the variability in drainage density and rate of network development [e.g., *Marani et al.*, 2003]. These data are plotted in Figure 10 and may help

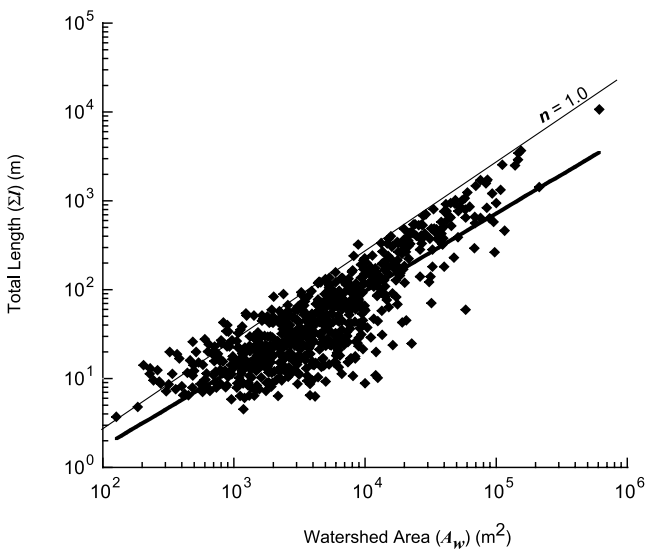

Figure 10. Total network length (Σl) versus watershed area (A_w). Regression $\Sigma l = 0.03A_w^{0.88}$, shown as a thick solid line, $r^2 = 0.85$. Upper limit with a slope of 1.0 is shown as a thin solid line.

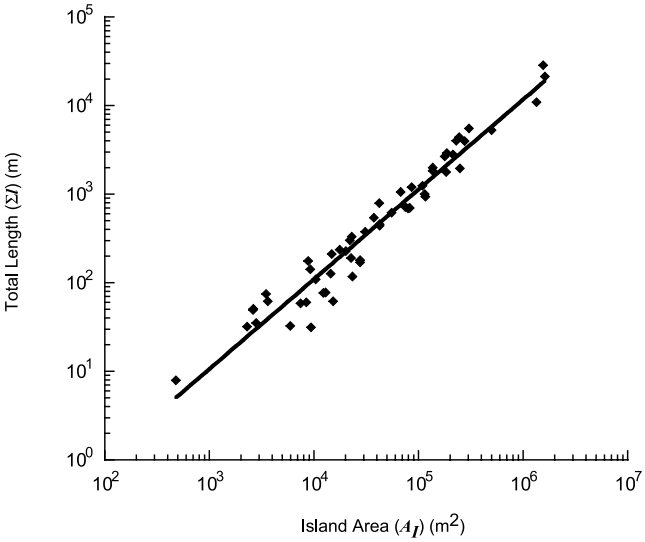

Figure 11. Total creek length on island (Σl) versus island area (A_I). Regression equation $\Sigma l = 0.009 A_I^{1.01}$, $r^2 = 0.91$.

visualize the extent of network dissection into the marsh platform. While scatter on this plot increases as area increases, for basins with area greater than ~2000 m^2 the upper limit to the plot defines a nearly straight line with a slope of 1.0. This means that for larger basins, total channel length can be expected to increase up to a predictable length determined by a power function with a unit exponent (Figure 10). Moreover, the positive regression through these data gives the power function $\Sigma l = 0.03 A_w^{0.88}$. The slope of the line, 0.88, is similar to the values reported by *Steel and Pye* [1997] and the assumed unit value of *Marani et al.* [2003]. Consistent with the concept that the island is the landscape unit of geomorphic analysis, the relationship between total channel length for each island versus island area was evaluated. Figure 11 depicts a power function with essentially a unit exponent. Both Figures 10 and 11 show the greatest degree of scatter for areas less than 10^4 m^2.

5. Discussion

[31] Results show that we cannot reject the hypothesis that marsh creek networks are topologically random. This result is consistent with the random topology of terrestrial networks [e.g., *Shreve*, 1969] and it provides a theoretical framework for the application of terrestrial concepts to the analysis of intertidal environments despite the different environmental conditions (e.g., bidirectional flow, cohesive sediment, diurnal bank-full stage). Hence terrestrial geomorphic concepts and analyses may provide insight on intertidal landscape development and stability. In this section we attempt to (1) provide an explanation for the observed similarities and differences in the structure of marsh versus terrestrial drainage networks and reconcile the wide range in drainage densities in the North Inlet basin and (2) justify the use of the marsh island as the unit of geomorphic analysis and provide an interpretation of the results of this analysis.

5.1. Tidal Versus Terrestrial Networks

[32] Salt marsh networks resemble those of terrestrial landscapes in that they are topologically random, obey Hack's law (mainstream length versus watershed area), and follow Horton's laws of numbers versus order and mean stream length versus order. These similarities suggest similar mechanisms for energy dissipation through their respective networks, one set by tidal range and the other set by rainfall accumulation and flow. They differ in that North Inlet marsh networks have substantially greater drainage densities, are more elongate and have shorter mean stream segment lengths for a give stream order.

[33] Since *Shreve* [1969] was able to derive both Hack's and Horton's laws from the axiom of topological randomness, it is not surprising that topologically random marsh networks should also follow these laws. It is perhaps also not surprising that marsh networks are topologically random as they lack the factors that could cause departure from randomness in terrestrial networks, unidirectional flow on steep slopes and bedrock structural controls on network geometry. The differences on the other hand are most likely due to much greater depth of tidal runoff as compared to terrestrial runoff [*Gardner and Bohn*, 1980]. At North Inlet for example, the mean depth of tidal inundation is approximately 0.5 m, which over the course of a year results in total tidal runoff of 350 m (750 tidal cycles × 0.5 m) as compared to typical terrestrial runoff of 0.1 to 1.0 m/yr. Thus tidal channels not only widen and deepen much more rapidly in the downstream direction than do their terrestrial counterparts, but they must also be more numerous to accommodate a large part of their significantly greater tidal fluxes.

[34] That the depth of the tidal runoff has an effect on marsh drainage density is further suggested by the following observations. Broad swaths of high marsh, such as those along the western margin of Goat Island and in the fringe marsh at the head of the Crab Haul Creek (Figure 1) are virtually devoid of tidal channels. Field observations indicate that the mean depth of inundation in these areas is on the order of a few centimeters as opposed to the low marsh areas east of Goat Island where mean depths of submergence are on the order of tens of centimeters. A similar contrast can be seen in the sparsely dissected *J. romerianus* marsh along the north margin of Mud Bay, several tens of centimeters higher in elevation than the *S. alterniflora* marsh to the north. Even within the lower lying *S. alterniflora* marsh, observations by the third author indicate that the marsh platform has a relief of approximately 0.2–0.3 m. These observations support the notion that in the North Inlet basin drainage density is related to the mean depth of tidal inundation and that the variations in drainage density shown on Figure 10 could be due to variations in the mean elevation of the basins studied. Given the higher drainage densities of marshes, the lower mean link lengths in marshes compared to terrestrial watersheds can be attributed to their need to fit more channels into a unit area in order to accommodate the large volume of tidal flow.

[35] Moreover, our results support the finding of *Marani et al.* [2003], that drainage density cannot reliably distinguish intertidal landscapes from terrestrial landscapes. A comparison of our Figure 10 to Figure 10 of Marani et al. shows more scatter about the ΣL versus A_w trend line for the North Inlet data. This scatter may result from the larger number of samples in the present data set, from the different methods used to determine watershed area or from uncer-

tainty in manual delineation of lengths. Alternatively, we speculate that the smaller basins (10^2–10^4 m^2) may have adjusted their total creek lengths to accommodate the greater influx of water attributed to sea level rise. This results in the scatter of points that lie above the n = 1.0 line on Figure 10, indicating that total channel length is increasing. Moreover, the scatter in these data largely is largely below the lower range of values reported by Marani et al. These observations indicate that the North Inlet intertidal watersheds are not characterized by a spatially uniform drainage density, unlike the results of Marani et al. We speculate that variations in drainage density in intertidal wetlands arise from variations in mean elevation among watersheds, and thus mainly are a function of the tidal prism. Accordingly, greater drainage density should facilitate the flood and ebb of tidal waters in lower lying marsh watersheds.

[36] At first glance this conclusion would seem to be at odds with the results presented by *Marani et al.* [2003] whose marsh watersheds showed little variation in drainage density, but significant regional variation in the relationship of total channel length to the volume of the tidal prism. In the Venice Lagoon, we hypothesize that the lower lying St. Felice basins have a larger tidal prism for a given total channel length than do the higher Pagliaga basins despite the fact that the regressions of total channel length versus basin area for the two systems are collinear and thus of uniform drainage density (e.g., unit slope of Marani et al.'s Figure 10). We reconcile this discrepancy in the following way: First, on the basis of our data and that of *Marani et al.* [2003], it appears empirically that there is an upper limit to the total channel length that can be accommodated by a given basin area which constrains the drainage density to a maximum value of about 0.025 m^{-1} (approximate y intercept of Figure 10 and Marani et al.'s Figure 10). Almost all of the basins in the Venice Lagoon are at or close to this limit whereas many of the basins in the North Inlet system fall substantially below it (Figure 10). We further hypothesize that it is not only total channel length that must adjust to the mean tidal prism but also total channel planform area, which is the product of total channel length by the mean channel width. This is because ease of flow into a marsh watershed at stages above bank-full does not depend solely on total channel length but rather on total planform channel area. In summary, we suggest that since marsh channel networks are topologically random they are free to take on a range of network structures within the constraints imposed by the empirical limit on drainage density and the total channel area required to accommodate the tidal prism.

5.2. Salt Marsh Islands

[37] We hypothesize that island boundaries should exert some control on the length of the networks it contains. Specifically, island shape should restrict the size of networks present on a given island. For example, given islands of equal area, a small area ratio, A', (long, narrow island) should maintain a correspondingly shorter maximum channel length, and a larger area ratio should support a larger maximum channel length. However, a plot of maximum mainstream length (L_{max}) and area ratio exhibits no general trend (Figure 8); hence island shape exhibits little control on mainstream length. This finding may be the result of timing of channel initiation on an island and competition for area between adjoining networks. Networks that begin to form at the same time as a result of the same tidal prism should expand onto the same amount of area. We would then expect the mainstream lengths of all the networks on the islands to be equal. However, depending on the island shape we may see islands with highly variable mainstream lengths. This suggests that networks forming next to each other may vie for neighboring space. If a network succeeds in garnering more space than its neighbors it can become the dominant network on an island. Also, variations in channel sinuosity may influence the elongation and expansion of networks on a given island and its drainage density.

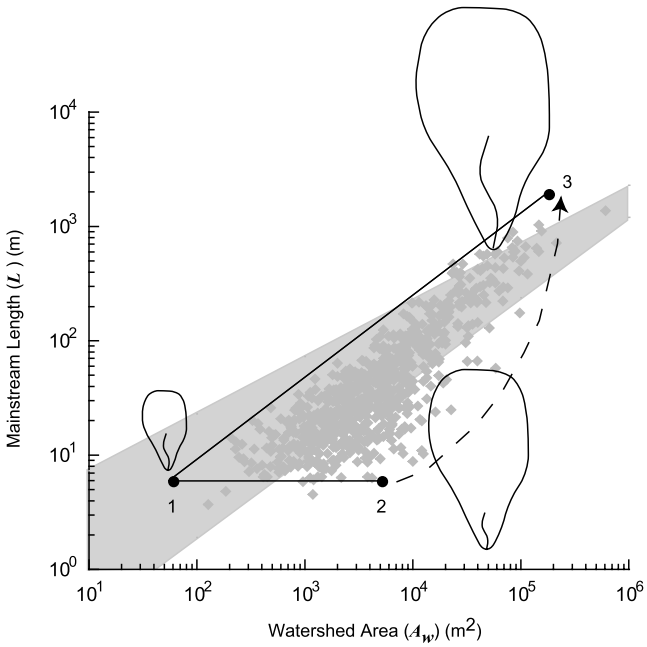

Figure 12. Mainstream length (L) versus watershed area (A_w). Points 1–3 illustrate hypothetical networks.

[38] Also, variations in the L-A_w relation (Figure 6) may be explained by variable sinuosity of the main channel, location of channel mouth relative to island shape or spatially and temporally variable incision by channels into the marsh platform. An envelope around the data in Figure 12 reveals three characteristic end-member L-A_w relationships. At point 1 in Figure 12 the end-member L-A_w relation depicts relatively small basin areas and mainstream lengths. Advancing horizontally to point 2 the mainstream lengths remain fixed but watershed area increases. In advancing from point 1 to point 3 however, both mainstream length and watershed area co-vary by the power function relation. We hypothesize as above that with increasing mean depth of submergence (i.e., area normalized tidal prism) L-A_w points will tend toward the line defined by points 1 and 3. Hence the spatially and temporally variable marsh dissection may ultimately lead to a characteristic L-A_w scaling. Likewise, the scatter in Figure 10, Σl-A_w, may arise for the same reasons as in Figure 6, variable sinuosity, channel mouth location and variable marsh incision rates. The sharp upper edge to the data for watersheds greater than ~2000 m^2 indicates that an upper limit to the dissection of the marsh watersheds may exist. Therefore, as argued for Figure 6, the total stream lengths that lie below the sharp break may tend toward this upper limit. The slope of this

upper limit is equal to 1.0. *Marani et al.* [2003] interprets a slope of 1.0 for a plot of total channel length and watershed area as an indication that surface processes dissecting the marsh landscape are spatially uniform.

[39] A similar relationship exists for total channel length and island area. For example, the power function fit to Σl-A_I data in Figure 11 gives a slope 1.01. We extend *Marani et al.*'s interpretation to suggest that processes operating at the island scale are spatially uniform or average out variation due to depth of inundation. Given the difficulty in defining individual watershed boundaries and corresponding watershed areas, we propose that in some marsh landscapes where larger channels define marsh islands, the marsh island should be the preferred unit of landscape for geomorphic analysis. Its boundaries are well defined and easily detected from a variety of remote sensing techniques. Therefore we may no longer need to define watershed areas in marsh environments using flow divide models.

[40] Finally, analyses and geomorphic parameterizations presented here provide a framework for assessing network features and comparison of these geomorphic indices to those developed in a relatively undisturbed marsh environment. Hence this work may help establish quantifiable indicators of salt marsh disturbance.

6. Conclusions

[41] The topologically random network model [*Shreve*, 1966; *Smart*, 1968] provides a theoretical framework for the explanation and prediction of drainage network composition. Results show that we cannot reject the hypothesis that North Inlet salt marsh creek networks are topologically random. This finding indicates that terrestrial concepts for analyzing channel network geometry may apply to the intertidal zone. Hortonian analyses show differences in the slopes between terrestrial and marsh networks indicating that terrestrial network extension may be much slower than marsh extension. This idea is supported by the magnitude and mean segment length data showing that a limit to channel segment length may exist for marsh networks. Length-area analyses show that marsh networks are more elongate than terrestrial networks, and relations between total stream length and watershed area and island area suggest that networks expand until they reach a total network length maximum. This maximum value is set by the observed unit gradient between total stream length and basin area and it indicates that network growth rates for islands may be uniform, while rates for watersheds tend toward a uniform growth rate.

[42] Because of the complexity of defining individual watershed boundaries and corresponding watershed area in the intertidal salt marsh, we propose that the marsh island should be the preferred unit of landscape for geomorphic analysis. Its boundaries are well defined and easily detected from a variety of remote sensing techniques and it precludes the arduous and sometimes arbitrary task of defining watershed or basin area.

[43] **Acknowledgments.** This research was funded by the NOAA NERRS Graduate Fellowship Program, NSF grant EAR 02-29358 and EPA grant R-828677. John Jensen and Steven Schill provided the ADAR imagery. John Grego provided insight on random probability theory. Sergio Fagherazzi, Jonas Almeida, and Alan James provided insightful comments.

References

Allen, J., and K. Pye (1992), *Saltmarshes: Morphodynamics, Conservation and Engineering Significance*, Cambridge Univ. Press, New York.

Brush, L. (1961), Drainage basins, channels, and flow characteristics of selected streams in central Pennsylvania, *U.S. Geol. Surv. Prof. Pap.*, *282-F*, 161–181.

Cleveringa, J., and A. Oost (1999), The fractal geometry of tidal-channel systems in the Dutch Wadden Sea, *Geol. Mijnbouw*, *78*(1), 21–30.

Collins, L., J. Collins, and L. Leopold (1987), Geomorphic processes of an estuarine marsh: Preliminary results and hypotheses, in *International Geomorphology: Proceedings of the First International Conference on Geomorphology*, part I, edited by V. Gardiner, pp. 1049–1072, John Wiley, Hoboken, N. J.

Fagherazzi, S., and D. Furbish (2001), On the shape and widening of salt marsh creeks, *J. Geophys. Res.*, *106*, 991–1003.

Fagherazzi, S., A. Bortoluzzi, W. Dietrich, A. Adami, A. Lanzoni, M. Marani, and A. Rinaldo (1999), Automatic network extraction and preliminary scaling features from digital terrain maps, *Water Resour. Res.*, *35*(12), 3891–3904.

Gardiner, V., K. Gregory, and D. Walling (1977), Further notes on the drainage density-basin area relationship, *Area*, *9*, 117–121.

Gardner, L., and M. Bohn (1980), Geomorphic and hydraulic evolution of tidal creeks on a subsiding beach ridge plain, North Inlet, South Carolina, *Mar. Geol.*, *34*, M91–M97.

Gardner, L. R., and W. Kitchens (1978), Sediment and chemical exchanges between salt marshes and coastal waters, in *Transport Processes in Estuarine Environments*, edited by B. Kjerfve, Univ. of S. C. Press, Columbia.

Gardner, L., and D. Porter (2000), Stratigraphy and geologic history of a southeastern salt marsh basin, North Inlet, South Carolina, USA, *Wetlands Ecol. Manage.*, *9*(5), 1–15.

Gardner, L., L. Thombs, D. Edwards, and D. Nelson (1989), Time series analyses of suspended sediment concentrations at North Inlet, South Carolina, *Estuaries*, *12*(4), 211–221.

Geyl, W. (1976), Tidal neomorphs, *Z. Geomorphol.*, *20*(3), 308–330.

Goñi, M. A., and K. A. Thomas (2000), Sources and transformations of organic matter in surface soils and sediments from a tidal estuary (North Inlet, South Carolina, USA), *Estuaries*, *23*(4), 548–564.

Hack, J. (1957), Studies of longitudinal stream profiles in Virginia and Maryland, *U.S. Geol. Surv. Prof. Pap., 294-B*.

Horton, R. (1945), Erosional development of streams and their drainage basins: Hydrophysical approach to quantitative morphology, *Geol. Soc. Am. Bull.*, *56*, 273–370.

Jensen, J. (2000), *Remote Sensing of the Environment: An Earth Resource Approach*, 544 pp., Prentice-Hall, Old Tappan, N. J.

Jensen, J., G. Olsen, S. Schill, D. Porter, and J. Morris (2002), Remote sensing of biomass, leaf-area-index, and chlorophyll a and b content in the ACE Basin National Estuarine Research Reserve using sub-meter digital camera imagery, *Geocarto Int.*, *17*(3), 25–34.

Kirchner, J. (1993), Statistical inevitability of Horton's laws and the apparent randomness of stream channel networks, *Geology*, *21*, 591–599.

Knighton, A., C. Woodroffe, and K. Mills (1992), The evolution of tidal creek networks, Mary River, northern Australia, *Earth Surf. Processes Landforms*, *17*, 167–190.

Langbein, W. (1963), The hydraulic geometry of a shallow estuary, *Int. Assoc. Sci. Hydrol.*, *8*, 84–94.

Leonard, L. (1997), Controls of sediment transport and deposition in an incised mainland marsh basin, southeastern North Carolina, *Wetlands*, *17*(2), 263–274.

Marani, M., E. Belluco, A. D'Alpaos, A. Defina, S. Lanzoni, and A. Rinaldo (2003), On the drainage density of tidal networks, *Water Resour. Res.*, *39*(2), 1040, doi:10.1029/2001WR001051.

Myrick, R., and L. B. Leopold (1963), Hydraulic geometry of a small tidal estuary, *U.S. Geol. Surv. Prof. Pap.*, *422-B*.

Pestrong, R. (1965), The development of drainage patterns on tidal marshes, Ph.D. thesis, Stanford Univ., Stanford, Calif.

Pethick, J. (1980), Velocity surges and asymmetry in tidal channels, *Estuarine Coastal Mar. Sci.*, *11*, 331–345.

Pethick, J. (1992), Saltmarsh geomorphology, in *Saltmarsh Geomorphology: Morphodynamics, Conservation, and Engineering Significance*, edited by J. Allen and K. Pye, Cambridge Univ. Press, New York.

Ragotzkie, R. (1959), Drainage pattern in salt marshes, in *Proceedings of the Salt Marsh Conference*, pp. 22–28, Mar. Inst., Univ. of Ga., Atlanta.

Redfield, A. (1972), Development of a New England salt marsh, *Ecol. Monogr.*, *24*(2), 201–237.

Rinaldo, A., S. Fagherazzi, A. Lanzoni, M. Marani, and W. Dietrich (1999a), Tidal networks: 2. Watershed delineation and comparative network morphology, *Water Resour. Res.*, *35*(12), 3905–3917.

Rinaldo, A., S. Fagherazzi, A. Lanzoni, M. Marani, and W. Dietrich (1999b), Tidal networks: 3. Landscape forming discharges and studies in empirical geomorphic relationships, *Water Resour. Res.*, *35*(12), 3919–3929.

Ritter, D., R. Kochel, and J. Miller (1995), *Process Geomorphology*, 545 pp., Wm. C. Brown, Dubuque.

Sharma, P., L. Gardner, W. Moore, and M. Bollinger (1987), Sedimentation and bioturbation in a salt marsh as revealed by ^{210}Pb, ^{137}Cs, and ^{7}Be studies, *Limnol. Oceanogr.*, *32*(2), 313–326.

Shreve, R. (1966), Statistical law of stream numbers, *J. Geol.*, *74*(1), 17–37.

Shreve, R. (1969), Stream lengths and basin areas in topologically random channel networks, *J. Geol.*, *77*(4), 397–414.

Shreve, R. (1974), Variation of mainstream length with basin area in river networks, *Water Resour. Res.*, *10*(6), 1167–1177.

Smart, J. (1968), Mean stream numbers and branching ratios for topologically random channel networks, *Bull. Int. Assoc. Sci. Hydrol.*, *13*, 61–64.

Steel, T., and K. Pye (1997), The development of saltmarsh tidal creek networks: Evidence from the UK, paper presented at Canadian Coastal Conference, Can. Coastal Sci. and Eng. Assoc., Guelph, Ontario.

Torres, R., M. Mwamba, and M. Goni (2003), Properties of intertidal marsh sediment mobilized by rainfall, *Limnol. Oceanogr.*, *48*(3), 1245–1253.

Tucker, G., F. Catani, A. Rinaldo, and R. Bras (2001), Statistical analysis of drainage density from digital terrain data, *Geomorphology*, *36*, 187–202.

Valdes, J., Y. Fiallo, and I. Rodriguez-Iturbe (1979), A rainfall-runoff analysis of the geomorphologic IUH, *Water Resour. Res.*, *15*(6), 1421–1434.

Vogel, R. L., B. Kjerfve, and L. R. Gardner (1996), Inorganic sediment budget for the North Inlet Salt Marsh, South Carolina, USA, *Mangroves Salt Marshes*, *1*(1), 23–25.

Wadsworth, J. (1980), Geomorphic characteristics of tidal drainage networks in the Duplin River system, Sapelo Island Georgia, Ph.D. Thesis, Univ. of Ga., Atlanta.

Willemin, J. (2000), Hack's law: Sinuosity, convexity, elongation, *Water Resour. Res.*, *36*(11), 3365–3374.

Wright, L., J. Coleman, and B. Thom (1973), Processes of channel development in a high-tide range environment: Cambridge Gulf-Ord River Delta, Western Australia, *J. Geol.*, *81*, 15–41.

Zeff, M. (1999), Salt marsh tidal channel morphometry: Applications for wetland creation and restoration, *Restoration Ecol.*, *7*(2), 205–211.

L. R. Gardner, K. I. Novakowski, R. Torres, and G. Voulgaris, Department of Geological Sciences, University of South Carolina, 701 Sumter Avenue, EWS 617, Columbia, SC 29208, USA. (kinovakowski@yahoo.com; torres@geol.sc.edu)

Figure 1. ADAR image shows location and geography of North Inlet. The study area is outlined in black.